Hindawi Publishing Corporation
International Journal of Aerospace Engineering
Volume 2016, Article ID 6531694, 11 pages
http://dx.doi.org/10.1155/2016/6531694

Research Article

Flow Characteristics Study of Wind Turbine Blade with Vortex Generators

Hao Hu, Xin-kai Li, and Bo Gu

Electricity Institute, North China University of Water Resources and Electric Power, Zhengzhou 450045, China

Correspondence should be addressed to Xin-kai Li; lxkncepu@163.com

Received 17 November 2015; Revised 8 March 2016; Accepted 16 March 2016

Academic Editor: Saad A. Ahmed

The blade root flow control is of particular importance to the aerodynamic characteristic of large wind turbines. The paper studies the feasibility of improving blade pneumatic power by applying vortex generators (VGs) to large variable propeller shaft horizontal axis wind turbines, with 2 MW variable propeller shaft horizontal axis wind turbine blades as research object. In the paper, three cases of VGs installation are designed; they are scattered in different chordwise position at the blade root, and then they are calculated, respectively, with CFD method. The results show that VGs installed in the separation line upstream, with the separation line of the blade root as a benchmark, show a better effect. Pneumatic power of blades increases by 0.6% by installing VGs. Although the effect on large wind turbines is not obvious, there is a space for optimization.

1. Introduction

With the stand-alone wind turbine efficiency increasing, the length of the rotor blades also gradually increased. For earlier wind turbine blades used to apply thinner airfoil, they were more likely to fracture when they were hit by a larger strength and load. Nowadays, thick airfoils are usually applied to the root of large-scale wind turbine blades to improve the structural strength of the blade. However, it is very easy for thick airfoil to generate flow separation, and the flow of the airfoil blade root is often off-design, which increases the possibility of flow separation. When flow separation occurs, it will have a negative influence on the efficiency of capturing wind power by wind turbines [1–4], so it gradually becomes a research hotspot in study of wind turbine aerodynamics to improve wind machine pneumatic efficiency by controlling the blade root flow separation.

Vortex generator (VG) is a representative of flow control measures, which was first promoted and applied to the aircraft wings by Taylor in the middle of the last century. Vortex generators are actually certain low aspect ratio wings vertically arranged on the surface of wind turbine blades. The two sides of winglet are pressure side and suction side, which can produce a wingtip vortex, and the aspect ratio is small; the strength of the wingtip vortex is bigger. High-energy wingtip vortex can promote the mixing of the fluid with high kinetic energy outside the boundary layer with low momentum fluid within the boundary layer and increase momentum and energy of the fluid within the boundary layer, so that the boundary layer separation is delayed or eliminated, with ultimately airfoil lift enhancement and drag reduction [5–9] realizing.

Nickerson Jr. [10], through the wind tunnel experiment, studied the change rule of drag characteristic of large wind turbine blade thick airfoils after adding vortex generator and found that the vortex generator can increase the lift coefficient of airfoils so as to achieve the purpose of improving lift-to-drag ratio. Gyatt [11] analyzed and studied small two-blade horizontal axis wind turbine installed with counterrotating vortex generators. There were three kinds of vortex generators arrangement—inner half-blade span, outside half-blade span, and the whole blade span. Measurement data in the wind field show that the installation of vortex generators can make the output power of wind turbines increase 20% with the coming flow wind speed of 10 m/s or more, the power drop less than 4% under the condition of low wind speed. In numerical simulation, in 2004, Johansen and others in their report of pneumatic, studied the influence of triangular

vortex generators on the blade aerodynamic performance [12]; and in 2005 they went ahead with the 3D calculation of VG installed on the wind turbine blades [13]. Liu et al. [14] explored the effect of the shape of vortex generators and arrangement and geometry size on airfoil flow separation through the method of numerical simulation and thus obtained the influence law of supercritical airfoil aerodynamic performance. In china, Zhang et al. [15] calculated the stall type wind turbine by simplifying the VGs to numerical model and using the method of NS equation added with the source term, and the results showed that the pneumatic VGs can make the turbine power increase by about 2%. At president, most research on the influence of VGs on wind turbine aerodynamic performance focuses on stall type of wind turbine, so it is urgent to explore the effect of VGs on aerodynamic performance of large variable propeller shaft and the applicability.

In this paper, three installation cases are put forward by analyzing the blade root flow condition at full wind speed, with CFD numerical simulation method and choosing 2 MW large variable propeller shaft wind turbine blade as research object. Meanwhile, a more reasonable blade spanwise installation position of VGs is given by comparing the calculated results got in the three cases.

2. Geometric Model and Numerical Method

2.1. Geometric Model. Figure 1 shows the blade geometry and VGs geometric model. Blade length is 45.281 m. The right part shows the shape and arrangement of VGs.

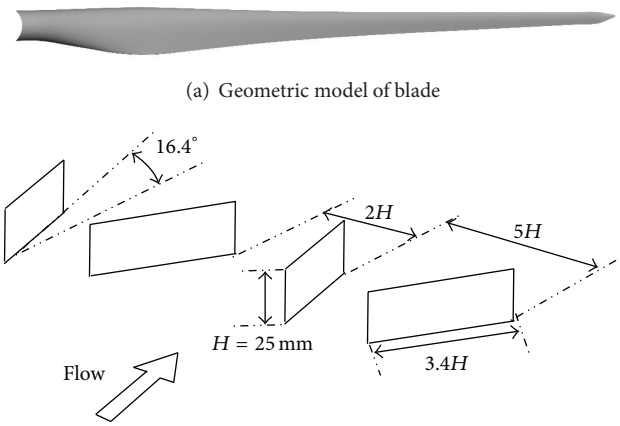

(a) Geometric model of blade

(b) Geometric model of VGs

Figure 1: Geometric model of blade and VGs.

2.2. Numerical Method

Mesh. The quantity and quality of mesh do have a great influence on CFD simulation results, so it is significant to ensure the comparison of the effects on blades with VGs and blades without VGs under the same grid. Therefore, in order to compare VGs effects on wind turbine aerodynamic performance in the same set of grid case, in this paper the boundary conditions (internal surface or no-slip wall) are changed. At first, this paper applies AutoGrid5 software to automatically generate blade whole grid and then subdivide VGs grids in the IGG, with grid number being about 10.5 million. Grid and boundary conditions are shown in Figure 2.

In this paper, CFD calculation is based on the commercial software Fine/Fine/Turbo™, with SA model as turbulence model and residual 10^{-5}. When the monitoring of torque as well as axial thrust monitored is nearly unchanged, it is thought that flow field has been convergent.

3. Analysis of Calculation Results

3.1. CFD Calculation Results of Clean Blades. Figure 3 shows DF93 wind turbine CFD calculation results compared with the design value; from Figure 3(a), the CFD calculation results can be seen under the most wind speed and there was good consistency between the design values. The wind turbine rated wind speed was 11 m/s, so after the rated wind speed wind machine adopts variable propeller constant speed control strategy to make the power output basically remain unchanged. Figure 3(b) shows the abscissa for the tip speed ratio, with longitudinal coordinates for power coefficient and dotted line in the figure as the Betz limit value. From Figure 3(b) low tip speed ratio can be seen and CFD calculation values are in good agreement with the design values, when the tip speed ratio and CFD calculation value and design value are slightly different, and in the high tip speed ratio CFD value and design value vary greatly. This is mainly due to the high tip speed ratio when the wind speed is low, lower than the power of the wind turbine, and blade flow is complicated now, and it is not easy for CFD to accurately predict the blade power.

Figure 4 shows the limit streamline of blade suction surface when DF93 wind turbine blades are at different wind speed. First of all, as can be seen from the figure, this kind of variable propeller shaft wind turbine, at the full wind speed, will generate larger flow separation at the blade root. In addition, because the wind turbine applies variable control strategy, blade root separation criterion is equivalent in the range of full wind speed. It provides a reference to the spanwise installation position of VGs by analyzing suction surface separation at the full speed.

Before studying VGs flow control, it is necessary to know about the flow situation of blade surface, so that more conducive measures to VGs installation and improvement measures can be proposed. Boundary layer separation of laminar flow has flow separation and turbulent separation, and the effect of VGs installation on the turbulent boundary layer is superior to the control effect of laminar flow [8], so this paper discusses transition condition of the blade under typical conditions as well. Figure 5 shows transition position and separation position of blade suction surface at three kinds of wind speed. From the figure, it can be seen that the transition position and separation position of the blade, under the three different conditions, are basically the same. And separation positions are all downstream of the transition position, which indicates that the separation of the blades at the blade root

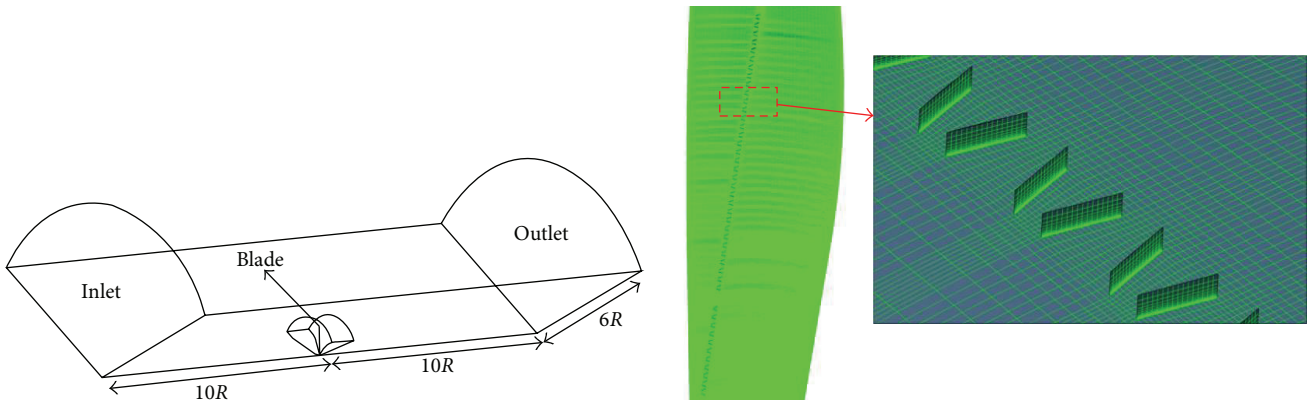

(a) Computational domain

(b) Mesh of blade and VGs

Figure 2: Computational domain of blades and the distribution of mesh.

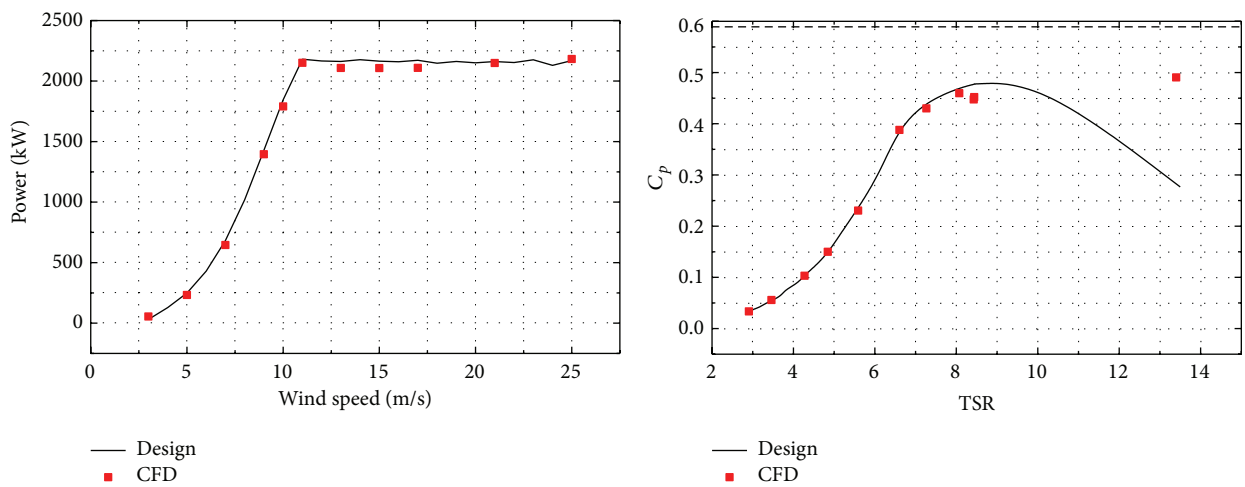

(a)

(b)

Figure 3: Simulation results between configuration of design and CFD. (a) Wind turbine power and (b) power coefficient.

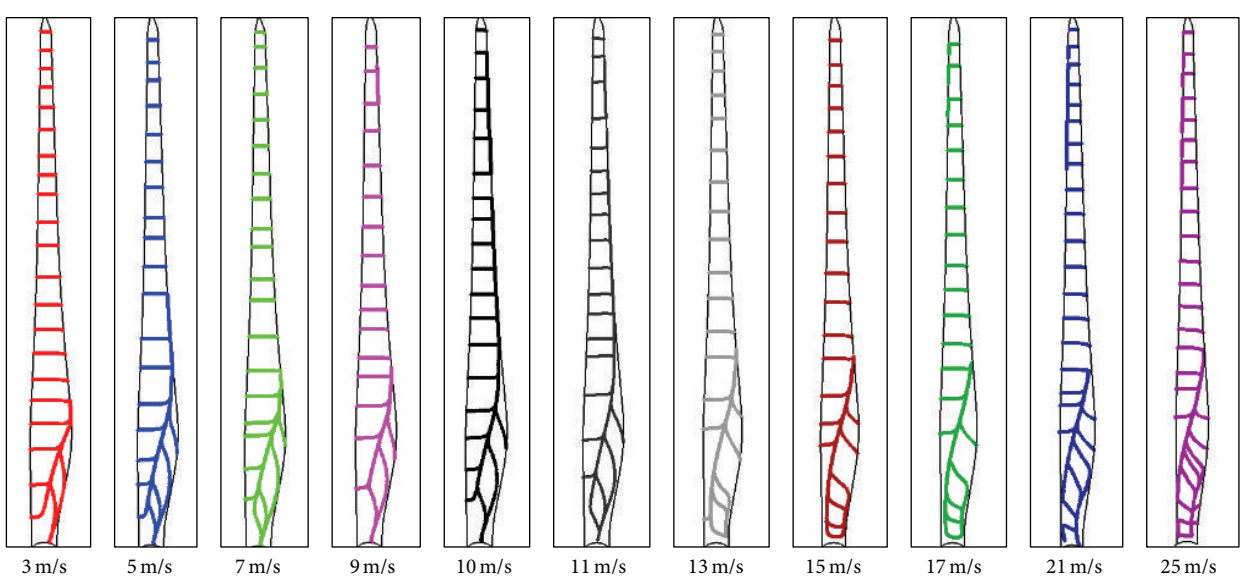

Figure 4: Blade surface limit streamline with velocity from 3 m/s to 25 m/s.

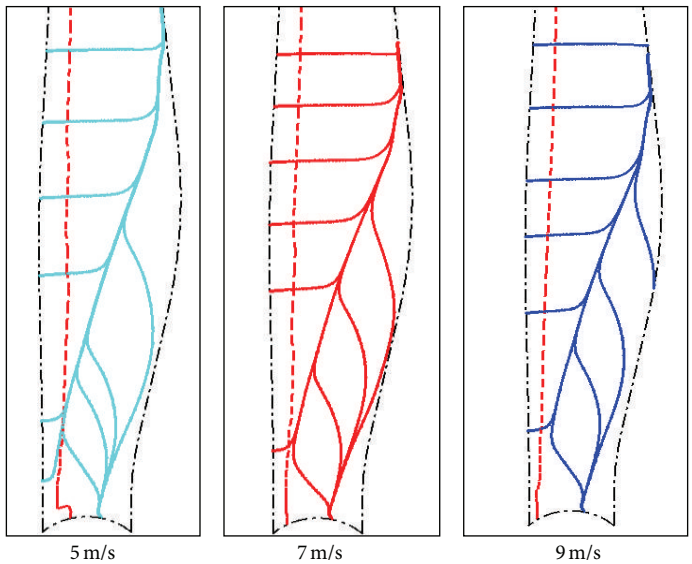

Figure 5: Blade surface transition line and limit streamline (solid line is the position of flow separation; dotted line is the position of transition).

is turbulent separation. Therefore, the study of the transition location and separation positon provides a reference to a chordwise installation position of VGs.

VGs incentive effect is closely related to boundary layer thickness of the local position; the greater H/δ (H is the height of VGs) is, the stronger vortex intensity generated by VGs is, while, at the same time, the greater resistance becomes. At present, the height of VGs is the same as thickness of the boundary layer when VG is used to control flow, so it is necessary to know about the change of boundary thickness of different spanwise and chordwise location at the blade root so as to provide a reference to design of VGs height. Figure 6 shows distribution of boundary thickness in different spanwise location at 9 m/s wind speed. In the figure, the maximum relative thickness corresponding to the seven spanwise locations from top to bottom is 0.35C, 0.4C, 0.5C, 0.6%, 0.7%, 0.8C, and 0.9C, respectively. It can be seen from the figure that boundary layer thickness from the blade leading edge to trailing edge becomes thick gradually, and the closer the cross section location is to the blade root, the thicker the boundary layer becomes.

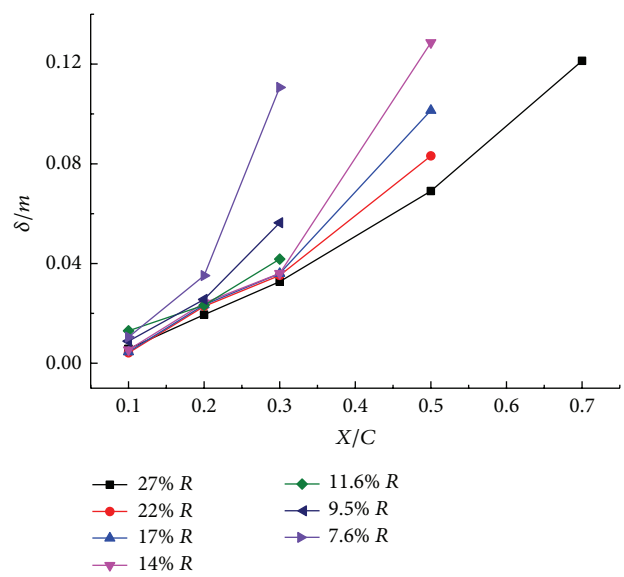

Figure 6: Thickness distribution along the boundary layer.

3.2. VGs Design Cases. (1) First of all, according to Figure 4, spanwise separation position of the blade suction surface at different wind speed is similar, so spanwise installation position of VGs ranges from 10% R to 27%.

(2) According to transition position at the blade root and chordwise separation position shown in Figure 5, three chordwise installation positions are selected, which is shown in Figure 7 detailedly. In case 1, transition position is chosen as a benchmark, and VGs are installed in 5H downstream of the transition location; the installation location is about 0.2C away from the blade leading edge. Case 3 chooses separate line as benchmark, and VG is put in about 30H upstream of the separation line. Case 2 is between case 1 and case 3, in which VGs are put about 10H away from the transition position downstream.

(3) The height of VG is closely related to the boundary layer thickness. Its height is determined according to Figure 6. Because the thickness of different spanwise and chordwise position at the blade root differs, in the paper three cases adopt the same VGs height for ease of comparison and analysis. In this paper, 0.025 m is taken as VGs height, H. Arrangement of VGs is shown in Figure 1, with VGs installation angle $\alpha = 16.4^{\circ}$.

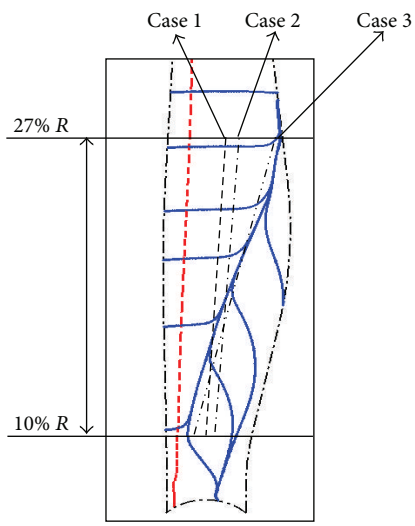

Figure 7: VGs installation position.

3.3. Calculation Results with VGs Blades. Figure 8 is the wind turbine power in three wind speeds when with or without VGs and power variation. Figure 8(a) shows that with the increase of the wind speed the power of the wind turbine increases, but the absolute value of the power with or without VGs change is not much. The power of case 1 in three wind speeds decreases slightly, and the remaining two cases of power generation increased slightly. Figure 8(b) is power increase value of blade with or without VGs; from Figure 8(b), in three wind speeds 5 m/s, 7 m/s, and 9 m/s, the power generation of case 1 has decreased, and the power decreased the minimum in 5 m/s, wind power decreased the maximum in 9 m/s, power decrease values into this relationship with wind speed were positive. For case 2, in three speeds 5 m/s, 7 m/s, and 9 m/s, the power values have increased with VGs, and at 7 m/s the power increased the maximum and power increased by 0.16%. For case 3, in 5 m/s, 7 m/s, and 9 m/s the same wind power has been increased, power increased with slightly lower values in 5 m/s, and in 9 m/s the power increased the most, the largest increase of power is 0.619%, and power increased with wind speed change basic linear relationship value. Contrasting the three VGs' scheme, for case 3 power increased more compared to case 2, and case 1 does not increase aerodynamic performance but also will fall in wind turbine power.

Figure 9 is annual energy production (AEP) of wind turbine with or without VGs (a) and the increase value of annual energy production (b). The graph abscissa is annual average wind speed, the annual energy production using the formula given in IEC (IEC61400-12-1). Generic AEP is estimated by applying the measured power curve to different reference wind speed frequency distributions. A Rayleigh distribution, which is identical to a Weibull distribution with a shape factor of 2, will be used as the reference wind speed frequency distribution. The AEP equation is

$$\mathrm{AEP} = N_h \sum_{i=1}^{N} \left[F\left(V_i\right) - F\left(V_{i-1}\right)\right] \left(\frac{P_{i-1} + P_i}{2}\right), \quad (1)$$

where AEP is the annual energy production; N_h is the number of hours in one year ≈8760; N is the number of bins; V_i is the normalized and averaged wind speed in bin i; and P_i is the normalized and averaged power output in bin i.

And

$$F(V) = 1 - \exp\left(-\frac{\pi}{4}\left(\frac{V}{V_{\mathrm{ave}}}\right)\right), \quad (2)$$

where $F(V)$ is the Rayleigh cumulative probability distribution function for wind speed; V_{ave} is the annual average wind speed at hub height; and V is the wind speed.

The summation is initiated by setting V_{i-1} equal to V_i − 0.5 m/s and P_{i-1} equal to 0.0 kW.

From Figure 9(a), along with the increase of the annual average wind speed, wind turbine power generation increased; at low wind speed (<6 m/s) AEP increased slope more, generating capacity of wind speed increases quickly, and in the high speed section (>6 m/s) slope decreases with increasing wind speed, increasing the generating capacity with the wind the slow; on the whole, the AEP with the change of average wind speed increases exponentially with VGs. The absolute value of wind turbine AEP is not much different with or without VGs; when wind speed is high, the absolute value of VGs blade with AEP increased gradually. Figure 9(b) shows the scheme in case 1 in different wind speed where AEP decreased; AEP decreased about 0.4%; in low wind speed, the AEP decreased slightly lower, while, in the high wind speed, the AEP decreased more. For case 1, the higher the wind speed, the more the power decrease. The AEP have increased in case 2 and case 3; the AEP of case 2 increased approximately 0.135%, and the AEP has nothing to do with increasing the value of the basic wind speed. The AEP of case 3 increased the most, the AEP increased about 0.581% and high wind speed annual energy production increased value slightly more, and small wind speed annual energy production increased with slightly lower values.

Figure 10 is the thrust of wind turbine and thrust increase value. From Figure 10(a) it is visible that to increase the force of wind wheel wind speed increases; the absolute value of wind wheel is nearly with or without VGs. The axial thrust decreases slightly in case 1, while case 2 and case 3 axial thrust are increased slightly. Figure 10(b) shows that the scheme of 1 in three wind speeds 5 m/s, 7 m/s, and 9 m/s, axial thrust decreased, 5 m/s axial thrust is decreased by 0.0487%, and in 9 m/s decreased by 0.2575%, and the change of axial thrust value is directly proportional to the wind speed and higher axial thrust is down more. In case 2 the axial thrust of scheme 3 has increased 2 in the 5 m/s and 7 m/s program, when the axial thrust is increased, which increased by 0.5282% and 0.5128%, two schemes in the wind speed

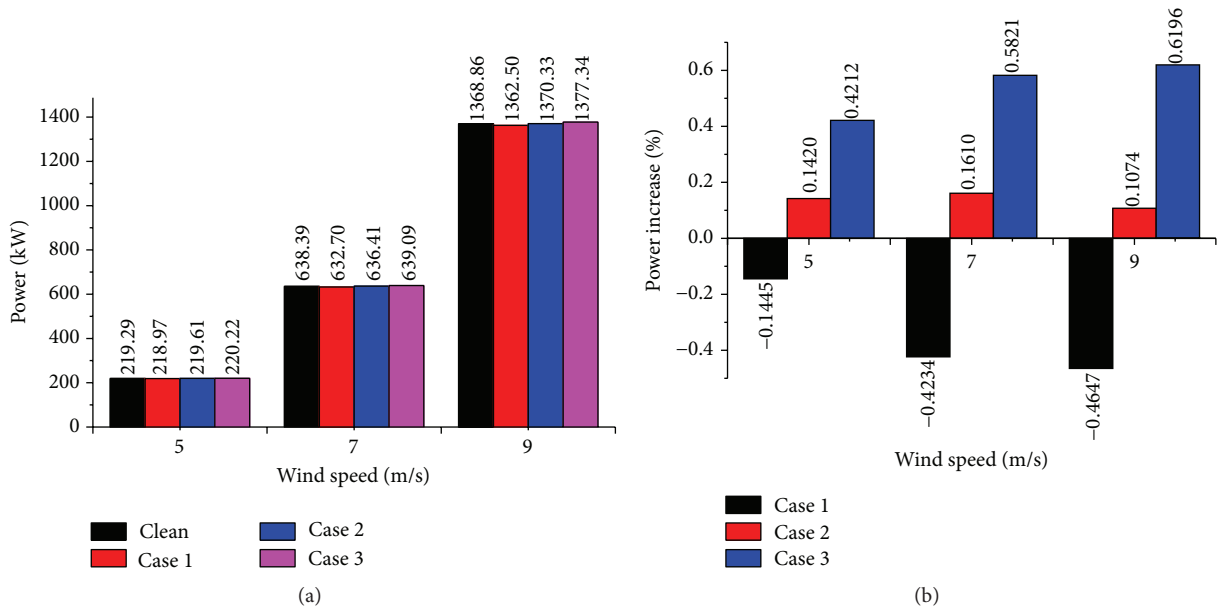

Figure 8: Wind turbine power and power increase value. (a) Power. (b) Power increase value.

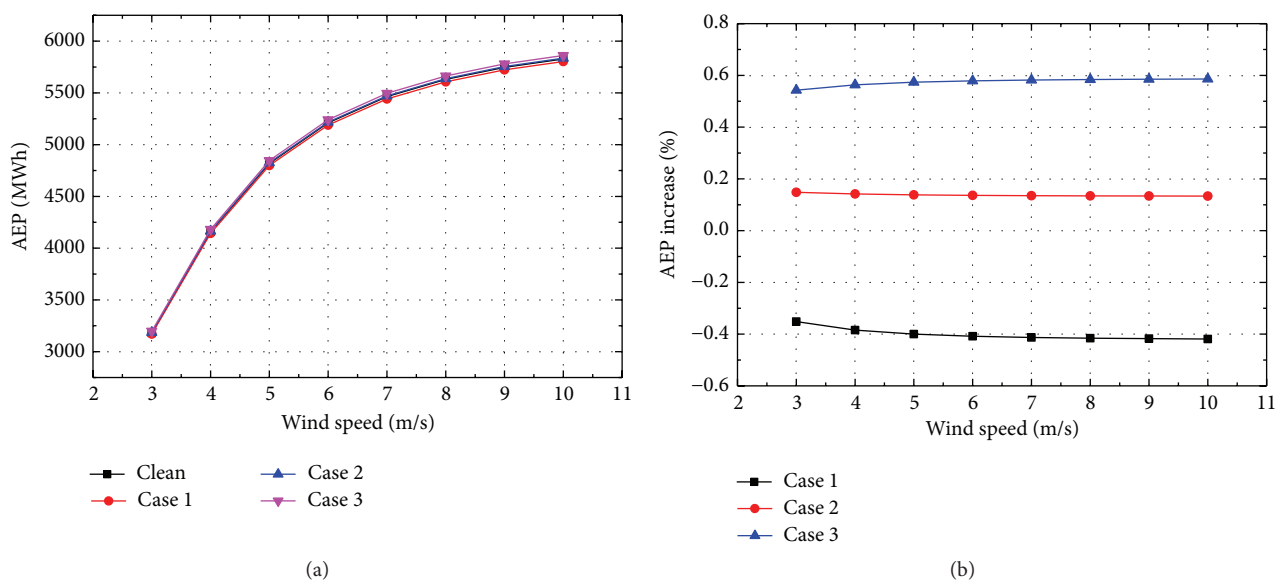

Figure 9: Annual energy production (AEP) and AEP increase value. (a) Annual energy production. (b) AEP increase value.

of case 2 compared to case 3 to increase the axial thrust. At 9 m/s, case 2 axial thrust is increased by 0.052%, while case 3 axial thrust increased plus 0.4288%.

Figure 11 is the wind wheel torque and torque variation. Figure 11(a) shows that the torque of wind wheel to the absolute value of the difference is not much with or without VGs; the torque of case 1 decreased slightly, while case 2 and case 3 torque increased slightly. From Figure 11(b), shows with or without VGs change in the torque value and Figure 8(b) shows no difference, because the power value is multiplied by the rotational speed and torques are obtained. Comparison of Figures 11(b) and 10(b) can be found to show that, in case 1, the torque is reduced while the axial thrust is reduced accordingly, variation of amplitude and velocity and the decline are suppressed, and the wind speed is high torque and axial thrust value declined more, while case 2 and case 3 are similar, while the increase of axial thrust torque will increase. And with wind speed torque increased higher, the axial thrust increase is also higher for case 3.

3.3.1. Streamline Analysis. The above is analysis of the impact of VGs on the wind turbine power; below we will analyze

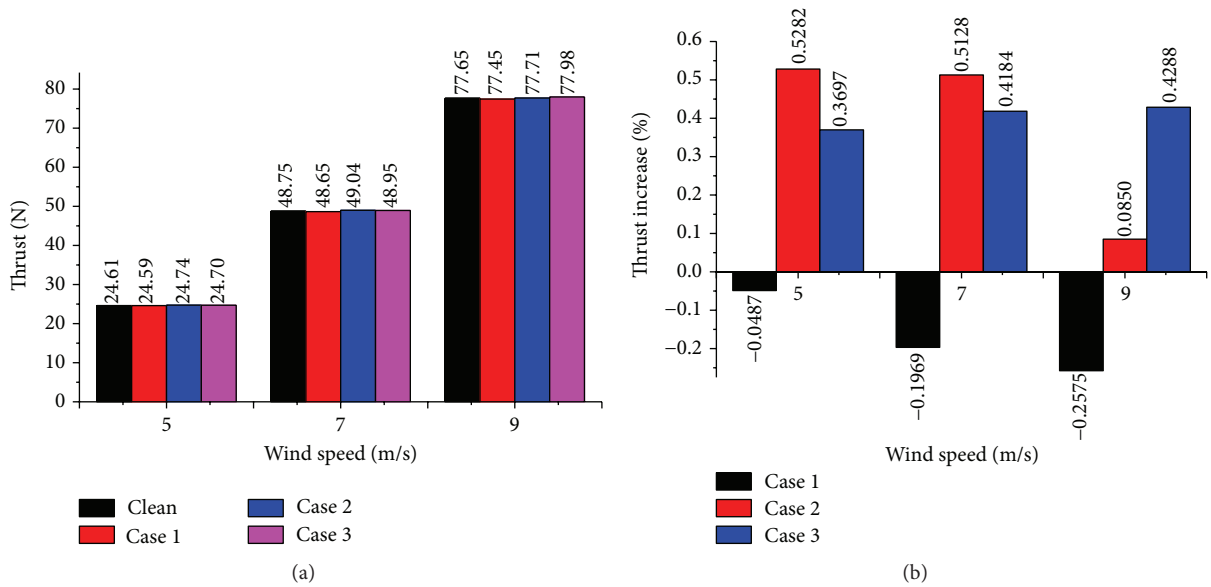

FIGURE 10: Thrust of wind wheel and thrust increase value. (a) Thrust. (b) Thrust increase value.

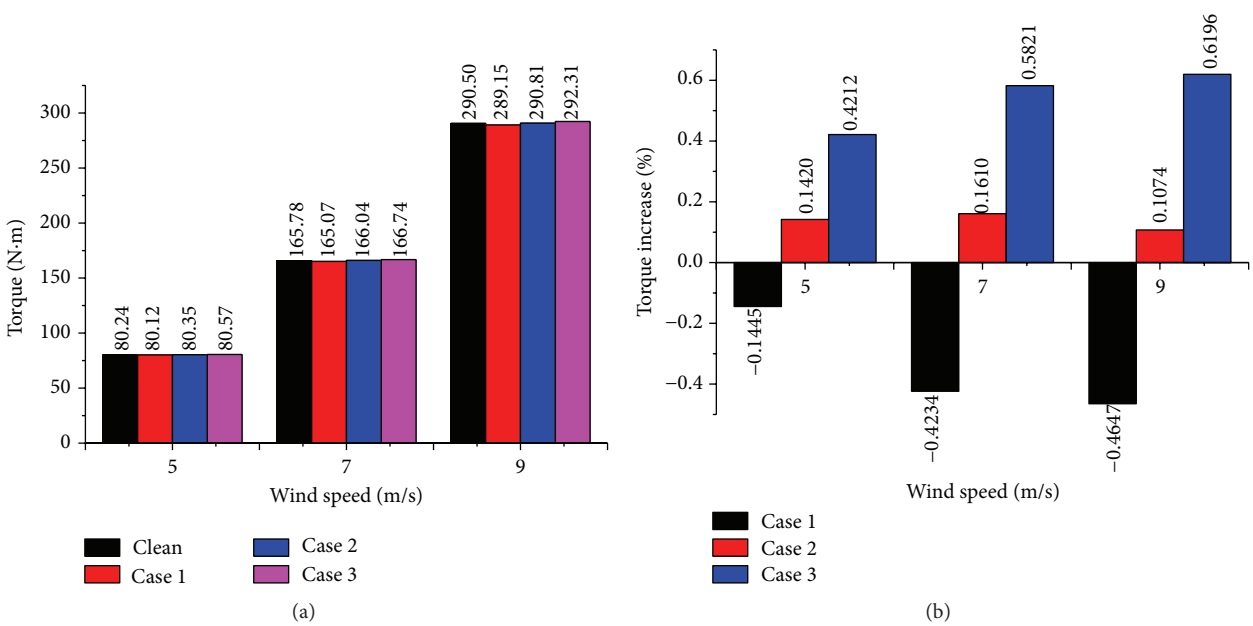

FIGURE 11: Torque of wind wheel and torque increase value. (a) Torque. (b) Torque increase value.

the flow field details, with analysis of the flow field to 9 m/s wind speed as an example analysis. Figure 12 shows three kinds of blade suction surface limit streamline and flow chart of cross section in three spanwise positions. The positions of the cross section are 17% R, 14% R, and 11.6% R, respectively, and the maximum relative thickness corresponding to them is 0.5C, 0.6C, and 0.7C, respectively. In the figure implementing line is for blades with VGs, and dotted line is for blades without VGs. As can be seen from the figure, in case 1 in three separation section locations of similar scale, VGs do not play the role of inhibition of flow separation; in case 2 trailing edge separation size with blades having VGs is reduced in the cross section of 17% R and 11.6% R, while the effect is not obvious in 14% R section; in case 3 in 1 and 3 cross sections VGs inhibit part of the flow separation, and the separation scale becomes smaller. From the comparison of limit streamlines of blade surface, case 3 can inhibit flow separation effectively.

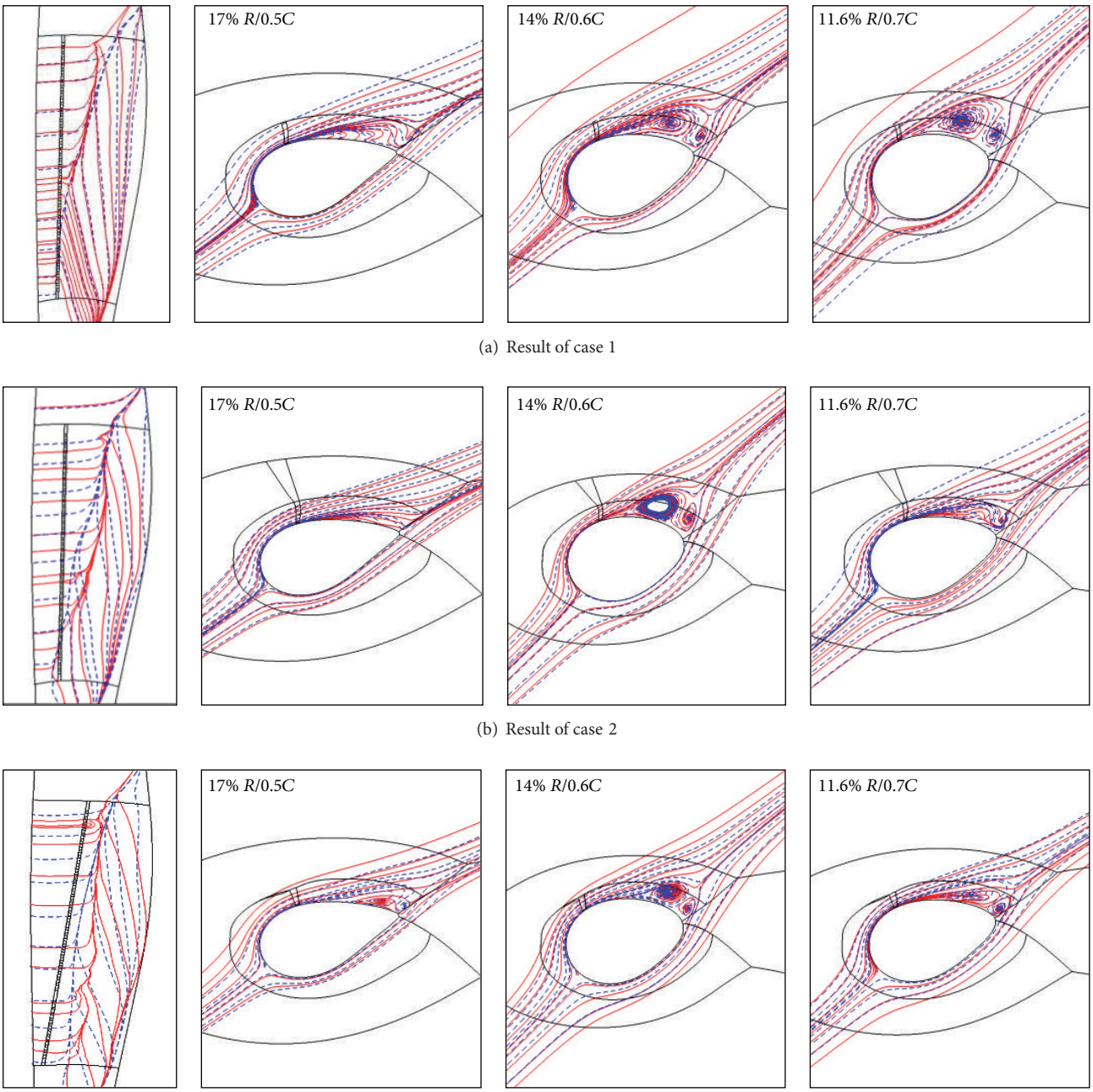

(a) Result of case 1

(b) Result of case 2

(c) Result of case 3

Figure 12: Limit streamline on the blade surface and spatial streamline (solid line: with VGs; dash-line: no VGs).

3.3.2. Pressure Coefficient. Figure 13 shows pressure distribution in the three cross sections. From the figure, pressure coefficient of the blade with VGs causes pressure jump (there is stress peaks and troughs), which is because the cross section is just located in VGs suction surface (pressure peak) or located in VGs pressure surface (pressure trough). As can be seen from plan 1 in 1 and 2 cross sections with VGs peak lower than the smooth blade, blade suction of plan 1 with VGs causes a smooth blade aerodynamic fall. For case 2 in 1 section some location in VGs surface pressure coefficient with no VGs is lower, but in some string to position 2 section pressure coefficient is higher than smooth blade change, with 3 basic cross section pressure coefficients, so plan 2 blade overall aerodynamic performance is largely unchanged. For case 3 in 1 and 2 cross sections suction side pressure coefficients are reduced, and solution 3 with VGs blade pneumatic power increases obviously.

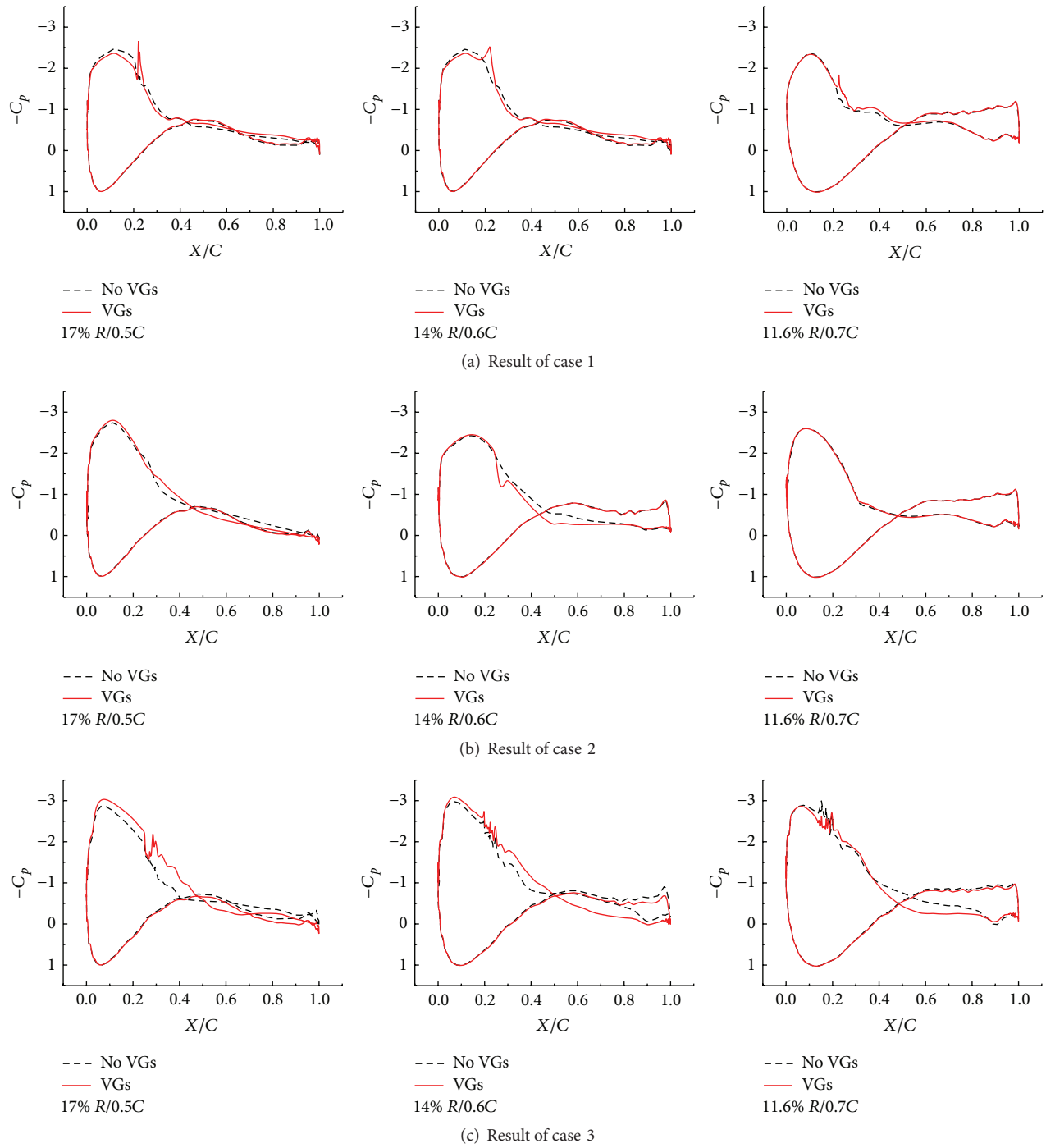

(a) Result of case 1

(b) Result of case 2

(c) Result of case 3

Figure 13: Pressure coefficient distribution on blade surface.

3.3.3. Analysis of Vorticity Contours. Figure 14 shows VGs downstream vorticity contour, and the distance between four sections and VGs(ΔX) is $1H$, $10H$, $20H$, and $30H$, respectively. From the figure, we can see that the conditions of downstream vortex flows in cases 1 and 2 are similar. In the upper blade span, vortex structures are not obvious when vortex moves to $30H$ downstream. In the lower blade span, vortex structures are not obvious when vortex moves to $10H$ downstream. In case 3, in the upper blade span vortex structures are not obvious when vortex moves to $20H$ downstream; however, in the lower blade span vortex moves a longer distance, and vortex structures remain when it moves to $30H$ downstream. Vortex distance is in the lower blade in comparison with it in the upper blade, which, in some degree, restrains development of vortex in span direction. It shows that it is inappropriate to adopt the same VGs arrangement in the lower blade span, and it is better to increase the distance of VGs in span direction.

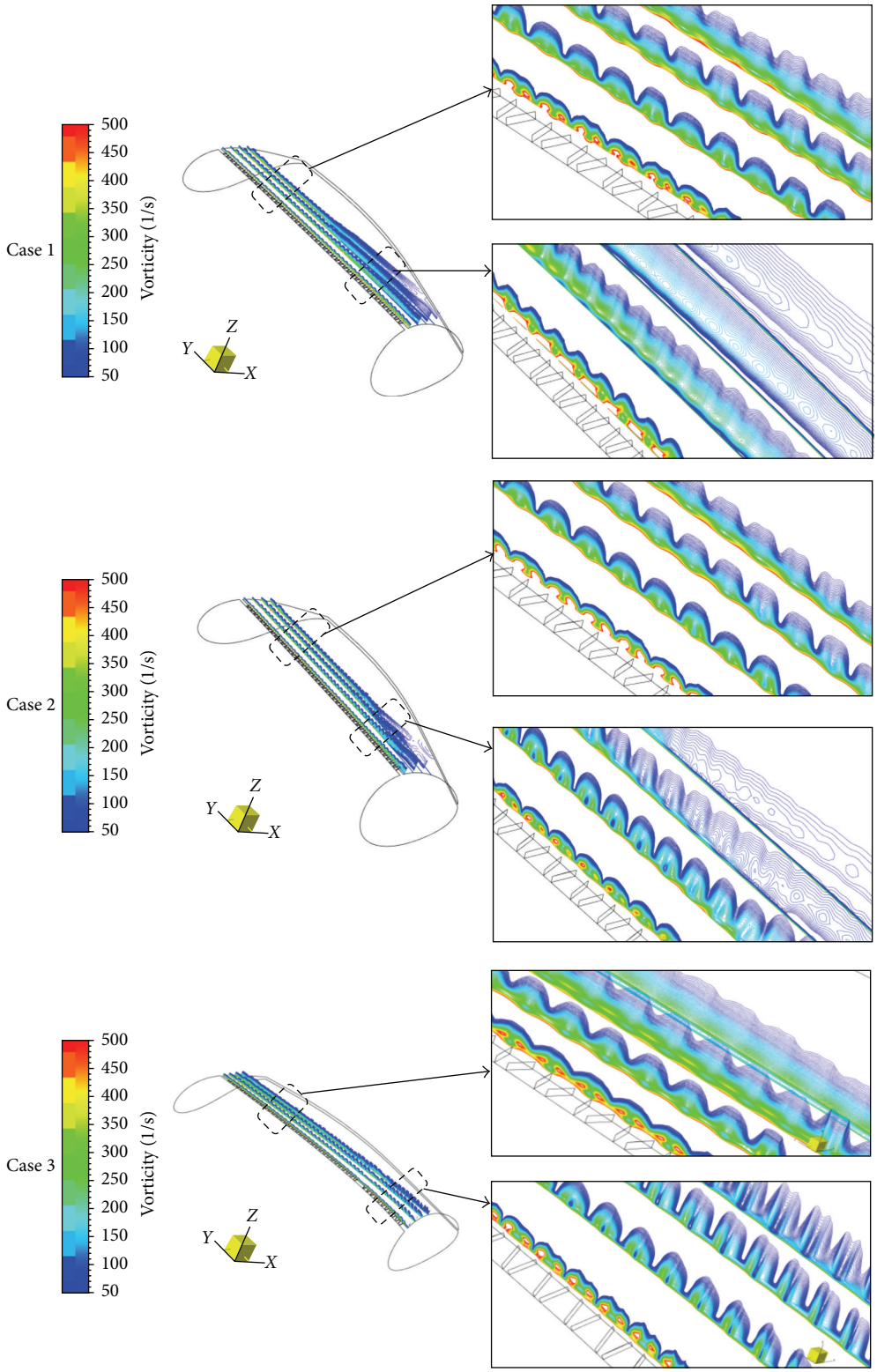

Figure 14: Distribution of vorticity contour downstream of VGs.

4. Conclusion

In this paper, numerical calculation, with CFD method, is done to smooth wind turbine blades and blades with VGs installed in three chordwise direction of blade root. Calculation results are as follows.

(1) For MW variable propeller shaft wind turbine, in the condition of the full wind speed, flow separation, in the suction side of the blade root, will occur and the separate scale is almost the same.

(2) Three different chordwise installation positions of VGs are designed according to transition line and separation line at the blade root. Calculation results show that the effect is the best and the blade pneumatic power increased by 0.6% or so, with VGs installed at its $30H$ upstream and separation line as a benchmark.

(3) It can be seen from the vorticity contour in different spanwise position of VGs downstream that it is not appropriate to install VGs with the same size in different positions of blades and in this chordwise position there is a space for optimization. It indicates that it is feasible to improve pneumatic power by applying VGs to large variable propeller shaft wind turbines.

Competing Interests

The authors declare that they have no competing interests.

Acknowledgments

This research was funded by Zhengzhou Provincial Key Science and Technology Projects (153PKJGG112) and Henan Provincial Key Science and Technology Projects (142102210059) and supported by Program for Innovative Research Team (in Science and Technology) in University of Henan Province (no. 16IRTSTHN017). This support is most gratefully acknowledged.

References

[1] F. Zhongyao, *Numerical Simulations of Steady and Unsteady Aerodynamics of Wind Turbines*, North China Electric Power University, Beijing, China, 2011 (Chinese).

[2] Z. Fan, S. Kang, and J. Wang, "The validate and research on 3D numerical simulation of the aerodynamic perormance of wind turbine blades," *Acta Energiae Solaris Sinica*, vol. 31, no. 3, pp. 279–285, 2010 (Chinese).

[3] Z. Lei, *Wind Turbine Blade with Blunt Traling-Edge and Improvements of its Aerodynamic Performance*, Institute of Engineering Thermophysics, Beijing, China, 2011 (Chinese).

[4] M. Make and G. Vaz, "Analyzing scaling effects on offshore wind turbines using CFD," *Renewable Energy*, vol. 83, pp. 1326–1340, 2015.

[5] S. L. Gai and S. D. Sharma, "Experiments on the reduction of base drag of a blunt trailing edge aerofoil in subsonic flow," *Aeronautical Journal*, vol. 85, no. 844, pp. 206–210, 1981.

[6] A. R. Paul, P. Ranjan, V. K. Patel, and A. Jain, "Comparative studies on flow control in rectangular S-duct diffuser using submerged-vortex generators," *Aerospace Science and Technology*, vol. 28, no. 1, pp. 332–343, 2013.

[7] S. Shun and N. A. Ahmed, "Wind turbine performance improvements using active flow control," *Procedia Engineering*, vol. 49, pp. 83–91, 2012.

[8] J. S. Chawla, S. Suryanarayanan, B. Puranik, J. Sheridan, and B. G. Falzon, "Efficiency improvement study for small wind turbines through flow control," *Sustainable Energy Technologies and Assessments*, vol. 7, pp. 195–208, 2014.

[9] L. O. Salviano, D. J. Dezan, and J. I. Yanagihara, "Optimization of winglet-type vortex generator positions and angles in plate-fin compact heat exchanger: response surface methodology and direct optimization," *International Journal of Heat and Mass Transfer*, vol. 82, pp. 373–387, 2015.

[10] J. Nickerson Jr., "A study of vortex generators at low reynolds numbers," in *Proceedings of the 24th Aerospace Sciences Meeting, Aerospace Sciences Meetings*, AIAA-86-0155, 1986.

[11] G. W. Gyatt, "Development and testing of vortex generators for small horizontal axis wind turbines," Tech. Rep. NASA-CR-179514, 1986.

[12] J. Johansen, N. N. Soerensen, F. Zahle et al., "Aerodynamic accessories," Tech. Rep. Risø-R-1482, Risø National Laboratory, Roskilde, Denmark, 2004.

[13] J. Johansen, N. Sørensen, M. Reck et al., "Rotor blade computations with 3D vortex generators," Tech. Rep. Risoe-R-1486, Risoe National Laboratory, Roskilde, Denmark, 2005.

[14] G. Liu, W. Liu, B. Mou, and Z.-Y. Xiao, "CFD numerical simulation investigation of vortex generators," *Acta Aerodynamica Sinica*, vol. 25, no. 2, pp. 241–244, 2007 (Chinese).

[15] L. Zhang, K. Yang, C.-W. Huang, Q. Liu, and J.-Z. Xu, "Parameters design of vortex generators based on numerical models," *Journal of Engineering Thermophysics*, vol. 33, no. 12, pp. 2084–2087, 2012 (Chinese).